Characterization of Real Multi-Correlator Outputs for SQM Performance Evaluation

Paul Thevenon, Ikhlas Selmi, Jihanne El Haouari, Nina Marino, Elodie Rames, Daniel Delahaye, Christophe Macabiau, Mikael Mabilleau

Characterization of Real Multi-Correlator Outputs for SQM Performance Evaluation

Paul Thevenon, *ENAC, Université de Toulouse*
Ikhlas Selmi, *ENAC, Université de Toulouse*
Jihanne El Haouari, *ENAC, Université de Toulouse*
Nina Marino, *ENAC, Université de Toulouse*
Elodie Rames, *ENAC, Université de Toulouse*
Daniel Delahaye, *ENAC, Université de Toulouse*
Christophe Macabiau, *ENAC, Université de Toulouse*
Mikael Mabilleau, *EUSPA*

BIOGRAPHIES

Dr Paul Thevenon graduated as electronic engineer from Ecole Centrale de Lille in 2004 and obtained in 2007 a research master at ISAE in space telecommunications. In 2010, he obtained a PhD degree in the signal processing laboratory of ENAC in Toulouse, France. From 2010 to 2013, he was employed by CNES, the French space agency, to supervise GNSS research activities and measurement campaigns. Since the July 2013, he is employed by ENAC as Assistant Professor. His current activities are GNSS signal quality monitoring and GNSS precise positioning algorithms.

Dr Ikhlas Selmi is currently part of the SIGnal processing and NAVigation (SIGNAV) research axis of TELECOM team at ENAC. She graduated as engineer in Telecommunication and Signal Processing from ESIEE. She received her Ph.D. in 2013 from Telecom SudParis on mitigating GNSS interference between indoor and outdoor signals. She is currently working on GNSS signal distortion generated by the satellite payload.

Jihanne El Haouari, **Nina Marino** and **Elodie Rames** are ENAC students majoring in space and aeronautical telecommunication systems. They are expected to graduate in 2022.

Pr Daniel Delahaye is the head of the Optimization and Machine Learning Team of the ENAC research laboratory and he also in charge of the research chair "AI for ATM and Large-Scale Urban Mobility" in the new AI institute ANITI in Toulouse. He obtained his engineer degree from ENAC and did a Master of Science in signal processing from the national polytechnic institute of Toulouse in 1991. His obtained his PhD in automatic control from the aeronautics and space national school in 1995 under the co-supervision of Marc Schoenauer (CMAPX) and did a post-doc at the Department of Aeronautics and Astronautics at MIT in 1996 under the supervision of Pr Amedeo Odoni. He started his career working at the French Civil Aviation Study Center (CENA) and move to ENAC in 2008. He got his tenure in applied mathematics in 2012. He conducts research on mathematical optimization and artificial intelligence for airspace design and aircraft trajectories optimization. He actively collaborates with MIT, Georgia Tech and NASA (USA) on development of Artificial Intelligence algorithms for air traffic management applications.

Dr Christophe Macabiau graduated as electronics engineer in 1992 from ENAC in Toulouse, France. Since 1994, he has been working on the application of satellite navigation techniques to civil aviation. He received his Ph.D in 1997 and has been in charge of the signal processing lab of ENAC from 2000 to 2012. He is currently the head of the TELECOM team of ENAC.

Mikael Mabilleau is a standardisation engineer on SBAS in the EGNOS exploitation team of the European GNSS Agency (GSA). Since his graduation as engineer from the French civil aviation school (ENAC) in 2006, he has been involved in GNSS standardization activity carried by the main civil aviation standardisation bodies such as the EUROCAE WG 62 on Galileo, RTCA Special Committee 159 on GPS and the ICAO Navigation System Panel in charge of ICAO standard. Mikael is involved in the evolution of GNSS concepts (ARAIM and SBAS L1L5) supporting the development of the associated standards (SARPs and MOPS) for use in aviation.

ABSTRACT

Signal Quality Monitoring is a process put in place in augmentation systems such as SBAS or GBAS to monitor potential signal distortions with high integrity that may be created by a satellite failure. It generally consists in the combination of several correlator outputs in so-called metrics, such as the single ratio metrics, the symmetric ratio metric or the double different metrics. To validate the compliance of a particular combination of metrics, it is necessary to validate the detection performance of an SQM process against every possible distortions of a Threat Space, in presence of typical errors affecting the metrics.

Usually, theoretical models are used in order to simulate the error affecting the correlator outputs and the metrics. However, those models cannot fully capture the diversity of the errors, such as the temporal correlation of multipath, or its effects on close correlator outputs. It is therefore of high interest to use real data collect in order to derive the models of the correlator output models, to validate the compliance of an SQM in operational conditions.

ENAC has put in place an automated data collect in order to observe the distribution of correlator output errors over a long period. Due to the large variation of the number of low-elevation satellites in a day, this scheduling task requires a specific process to collect as many observations as possible from low-elevation satellites in a limited period of time. An optimization algorithm, adapted from the simulated annealing process, allows to find an optimal scheduling, taking into account the constraint of the long post-processing task of the collected digitized samples by a software receiver.

By accumulating a large set of correlator outputs from low-elevation satellites, an accurate distribution of the covariance matrix of the correlator outputs is obtained, capturing all the effects occurring in the real world and in a real receiver. Applying this distribution in the SQM compliance test can help to have a more realistic performance. The comparison of an SQM performance between theoretical and observation-based models shows some major differences.

INTRODUCTION

In order to protect a Civil Aviation user from a Hazardous Misleading Information (HMI) created by a non-nominal GNSS signal distortion [1], specific monitors, called Signal Quality Monitors, are implemented in SBAS (Satellite Based Augmentation System) [4], [6] and GBAS (Ground Based Augmentation System) [8], [9] systems. These monitors are based on the combining of different correlator outputs computed by the fixed SBAS/GBAS reference station receiver in order to detect the presence of signal distortions on the correlation function. As for any detection method, the detection threshold has to take into account the random error characteristics of the observables [6], [12]. In the SQM case, the sources of the random error affecting the multiple correlator outputs are the receiver noise and the multipaths. If these error sources are not accurately characterized, the performances of SQM will be degraded, by having frequent false alarms (higher than the authorized false alarm probability in SBAS/GBAS) or poor detection performance (lower than the detection performance defined by the required missed detected probability in SBAS/GBAS).

ENAC has set up a software receiver connected to choke ring antenna to collect multi-correlator outputs from GPS and Galileo signals. An automated process is used to collect and post-process data of received GNSS signals in order to maximize the number of collected samples during the data collect time while taking into account the used equipment's limitation (required post processing time and available storage space). ENAC's aim is to obtain several dozens of hours *(note to reviewers: the exact length will be updated in the final paper)* of correlator outputs data focused on satellites received at low elevation. To evaluate SQM performance with enough conservative margin (in term of false alarm and missed detection requirements), only data received from low elevation (between 5 and 10°) satellite are collected and processed.

This paper aims at characterizing the standard deviation, cross-correlation and time correlation of the random error affecting the collected correlator outputs, with the following structure. The first section will remind the underlying detection theory principles and the most common Signal Quality Monitoring (such as SQM2b), including the combination of correlator outputs, the smoothing process and the expected performances for a given C/N0. This section will put in evidence the importance of correctly characterizing the correlator outputs distribution for low elevation satellites. The second section will describe the experimental set-up installed at ENAC site with a particular focus on the automated planification which is based on an innovative optimization process. The third section will provide the analysis of the data collect, including standard deviation of the multi-correlator outputs' error, the correlation coefficients between the different correlator outputs and their time correlation constant. The fourth section will provide some illustration of the importance of correctly taking into account the random error characteristics, by comparing SQM performances

with correct or incorrect models of the correlator output distribution. The paper will conclude on the importance of such characterization and on the opportunities to improve SQM techniques based on real data collect.

SIGNAL QUALITY MONITORING THEORY AND APPLIED METHODS

Signal Quality Monitoring Principle

Evil Waveforms (EWF) are non-nominal distortions that can be observed on satellite signals and cause additional bias on the estimated user position. A Threat Model (TM) has been proposed by ICAO for GPS L1 C/A to describe the possible distortions that can be observed on the GPS signals [1]. A Threat Space (TS) is also proposed to define the EWF that can induce hazardous effect on SBAS user.
ICAO proposed three types of failures that could be related to payload functions, to the observed EWF event of 1993, and that would result in at least one of the three problematic effects on GPS L1 C/A receivers [1]:

- Threat Model A (TM-A) consists of the normal C/A code signal except that all the positive chips have a falling edge that leads or lags relative to the correct end-time for that chip. This TM is associated with a failure in the navigation data unit, the digital partition of a GPS or GLONASS satellite. This type of failure results in the creation of a flat zone at the top of the correlation function.
- Threat Model B (TM-B) introduces amplitude modulation and models the degradations in the analog section of the GPS or GLONASS satellite. More specifically, it consists of the output from a second order system when the nominal C/A code baseband signal is the input. TM-B assumes that the degraded satellite subsystem can be described as a linear system dominated by a pair of complex conjugate poles. These poles are located at $\sigma \pm j2\pi f_d$, where σ is the damping factor in unit of MNp/s and f_d is the resonant frequency in unit of MHz. This type of failure results in the creation of false peaks and distortions
- Threat Model C (TM-C) introduces both lead/lag and amplitude modulation. Specifically, it consists of outputs from a second order system when the C/A code signal at the input suffers from lead or lag. This waveform is a combination of the two effects described above.

These 3 threat models were endorsed by ICAO for GPS L1 C/A. As it can be understood, they depend upon 3 parameters:

- Δ representing the lead or lag relative to the correct end-time of the chip preceding the falling transition
- σ and f_d representing the second order system creating the amplitude modulation of the chip

A similar model has been proposed for Galileo signals. The Galileo E1c and E5a TS has been defined in [5] as presented in Table 1. The choice of the range of values of these parameters should then be performed to define a so-called Threat Space that is representative of the feared events. In this paper, we will only focus on signal distortions affecting the Galileo signals.

Table 1 – Galileo EWF Threat Space [5]

		Δ (µs)	σ (MNp/s)	f_d (MHz)
TM-A	Galileo E1c	[-0.12 0.12]	-	-
	Galileo E5a	[-0.1 0.1]	-	-
TM-B	Galileo E1c	-	[0.1 63]	[0.1 18]
	Galileo E5a	-	[0.1 23]	[0.1 8]
TM-C	Galileo E1c	[-0.12 0.12]	[0.1 63]	[0.1 18]
	Galileo E5a	[-0.1 0.1]	[0.1 23]	[0.1 8]

Signal Quality Monitoring (SQM) is put in place in augmentation systems such as SBAS or GBAS to monitor those distortions. As all these distortions will result in a deformation of the cross-correlation function between the received signal and a local replica of the theoretical signal from a particular satellite computed within a receive, SQM traditionally combines several correlator outputs in order to form several metrics, such as simple ratio (SR) metrics, symmetric difference ratio (SDR) metrics or double difference ratio (DDR) metrics:

$$M_{sr} = \frac{I_x}{I_0}, \qquad M_{sdr} = \frac{I_x - I_{-x}}{I_0}, \qquad M_{ddr} = \frac{(I_x - I_{-x}) - (I_y - I_{-y})}{I_0}$$

where I_x is the correlator output located x chip away from the prompt correlator, I_0 being the prompt correlator outputs.

Performance Evaluation of Signal Quality Monitors

Once a metric is computed, we can verify its compliance with regards to integrity requirements by comparing its deviation from the nominal (distortion-free) case to a compliance threshold. This test is performed for each single distortion i of the EWF threat space.

$$Test_M^i = \frac{M^i - M^{nominal}}{threshold_M^i}$$

A combination of metrics is able to detect a particular distortion i with the required performances if among all the metrics, at least one has $Test_M \geq 1$.

Finally, a formulation of the compliance threshold is necessary to complete the compliance evaluation process. The threshold is given by the following formula:

$$threshold_M^i = \left(k_{md}^i + k_{fa}\right)\tilde{\sigma}_M$$

where k_{fa} is the multiplier obtained from $P_{fa} = P_{fa}^{req}/N_M$ is the required false alarm probability allocated to a single metric P_{fa}.
$P_{fa} = P_{fa}^{req}/N_M$, where N_M is the number of metric and $P_{fa}^{req} = 1.5 \times 10^{-7}$, as defined in [10]
k_{md}^i is the multiplier obtained from the required missed detection probability. It is defined for each distortion i, depending on its impact on the differential pseudorange error induced by the distortion and other integrity parameters, as proposed in [10]. In this paper, only the rising scenario is considered, which impacts the considered value of k_{md}^i.
$\tilde{\sigma}_M$ is the standard deviation of the metric after different smoothing processes

In this study, the overall SQM process is composed of all combinations of SR, SDR and DDR metrics formed from the correlator outputs taken at the delays provided in Table 2.

Table 2 – correlator output delays used in the considered SQM process

	Correlator output delays (chips)
Galileo E1-C	± [0.02 0.03 0.04 0.06 0.08 0.1]
Galileo E5a-Q	± [0.2 0.4 0.6 0.8 1]

In order to verify the compliance of SQM with the requirements, it is necessary to compute the standard deviation of each smoothed metric $\tilde{\sigma}_M$.

Let us consider that we have a vector $\boldsymbol{I}$ of all the correlator outputs mentioned in Table 2, normalized by the prompt correlator. Each SQM metric M can be formed as a linear combination of elements of $\boldsymbol{I}$:

$$M = \boldsymbol{S}_M^T \boldsymbol{I}$$

Consequently, the standard deviation of M – before any smoothing process – can be obtained from the covariance matrix of $\boldsymbol{I}$, noted $\mathbf{C}_{\boldsymbol{I}}$, through the following formula:

$$\sigma_M = \sqrt{\boldsymbol{S}_M^T \mathbf{C}_{\boldsymbol{I}} \boldsymbol{S}_M}$$

In practice, the correlator outputs are processed in order to reduce the noise affecting them. A metric smoothing filter is put in place to reduce non-time-correlated noise (such as thermal noise), and the average from different receivers is taken to reduce non-space-correlated errors (such as multipath).
The resulting standard deviation of the smoothed metric is therefore

$$\tilde{\sigma}_M = k_{smth} k_{avg} \sigma_M$$

where k_{smth} provides the gain due to the metric smoothing filter
k_{avg} provides the gain due to the averaging operation between several receivers

In previous works [10], the standard deviation of the metrics was derived from

- the covariance of $\boldsymbol{I}$ was obtained through a theoretical model of the standard deviation of the correlator outputs at $C/N_0 = 30$ dBHz, considering a total integration time of $T_I = 1$ s. In particular, the off-diagonal elements of $\mathbf{C}_{\boldsymbol{I}}$ are assumed to

follow the ideal shape of the correlation function, and the diagonal elements are taken from a formula assuming only thermal noise [11]
- assuming a 25-s running average filter
- assuming a metric averaging between 4 receivers

These assumptions resulted in the values collected in Table 3.

Table 3 – Models for simulated correlator output

Parameter	Value	Note
$\sigma_{\boldsymbol{I}}$	$\left\|\frac{\mu_x}{\mu_0}\right\|\sqrt{\frac{1}{\mu_x^2}+\frac{1}{\mu_0^2}-2\frac{R_c(x)}{\mu_x\mu_0}}$	Theoretical formula comes from [11] where $\mu_x=\sqrt{2\frac{C}{N_0}T_I}R_c(x)$ $C/N_0=30$ dBHz $T_I=1$ s $R_c(x)$ is the GNSS signal autocorrelation function
k_{smth}	$1/1.5$	for a 25-s running average filter pessimistic assumption to account for unmodelled multipath [7]
k_{avg}	$1/\sqrt{4}=1/2$	averaging between 4 receivers
$\tilde{\sigma}_{\boldsymbol{I}}$	$k_{smth}k_{avg}\sigma_{\boldsymbol{I}}$	smoothed correlator outputs standard deviation

In practice, those assumptions may be challenged at different levels:
- multipath may be present due to obstacles around the receiver's antenna. This may lead to
  - a modification of the diagonal elements of $\mathbf{C}_{\boldsymbol{I}}$, due to inflation of the variation compared to the case when only thermal noise is considered
  - a modification of the off-diagonal elements of $\mathbf{C}_{\boldsymbol{I}}$, due to the cross-correlation between the correlator outputs introduced by the multipath
  - a modification of the smoothing gain, due to the temporal correlation of multipath error
- the tracking of low elevation satellites may result in particular behavior of the receiver
- the C/N_0 of the tracked satellites at low elevation may be different from the assumed 30 dBHz due to the receiver antenna, acquisition or tracking loop design.

It is quite difficult to model those different phenomena from a theoretical point of view, which led us to the requirement of having access to long data collect to be able to derive the smoothed correlator output covariance matrix from real observations. Due to the particular needs of this data collects, a software receiver has been used, in order to be able to obtain the numerous desired correlator outputs for the Galileo E1-C and E5a-Q signals.

One drawback of software receiver is the long duration for post-processing when lots of computation are desired, which prevents the software receiver from working in real-time and thus limits the availability of observations over a period. To mitigate this issue, an effort was put on the optimization of data collect planning and its automatization, in order to be able to collect as many data as possible, while taking into account the limitation due to the long post-processing step after each data collect.

OPTIMIZATION-BASED DATA COLLECT PLANNING

Penalty methods overview and application to scheduling problems

A constrained optimization problem (P) can be formulated as follow:

$$\begin{aligned}(\mathrm{P}):\quad &\min_{x} && f(x)\\ &\text{subject to} && g(x)\leq 0\\ & && x\in\mathbb{R}\end{aligned}$$

The penalty method is a popular and well-known optimization method for solving constrained problem such as (P). The aim is to transform a constrained optimization problem into a problem without constraints. It transforms (P) into another problem called (P')

by adding to the objective function in (P), a term called penalty function. This term consists in the multiplication of a penalty parameter by a measure of violation of the constraints. It can be modelled as follow [13]:

$$(\mathrm{P}'): \quad \min_{x} \quad f(x) + c \times p(x) \qquad x \in \mathbb{R}$$

Where c is the penalty parameter and $p(x)$ a function that represents a measure of violation.

As explained in [14], it is important to have suitable penalties in such a way that in the end of the algorithm, the penalty function cancels out. Then, the global minimum of the penalty function (P') will correspond to a constrained global minimum of (P).

There are different kind of penalty functions that can exist. Indeed, in (P'), the penalty function has an additive form, however, even though it is less seen in the literature, multiplicative penalty forms exist.

Furthermore, as described in [9] there are several different penalty functions, such as the death penalties, the static penalties, dynamic penalties, or adaptive penalties, that can be used. The death penalties are the simplest functions possible as they reject any unfeasible solutions by penalizing them with infinity. However, as suggested in [16], they are not suitable for solving any challenging problem. Then, static penalties were developed. They are more advanced as they apply constant penalties to unfeasible solutions and then enable to explore infeasible regions. However, the penalty parameters applied are constant and do not depend on the different iterations or generations like the dynamic penalties which have penalty parameters that are modified and dependent on the current generation number. Finally, the adaptive penalties are part of the dynamic method and their penalty parameters are updated for every generation and they dynamically adapt themselves according to the information gathered.

In [15] and [16], it is seen that stochastic metaheuristics, such as Genetic Algorithms (GA) but also Particle Swarm Optimization (PSO), Ant Colony Optimization (ACO) or Simulated Annealing (SA), are very suitable methods to be applied to solve this kind of problems and to find global optimal solutions.

Global optimization problems are very important and frequently encountered in engineering application according to [17] and the constraints of these problems are often dealt with a penalty technique. Indeed, many well-known problems depend on penalty functions. In general, the penalty parameter is to be updated along the iterative process so that the solution can be found faster. However, it is suggested in [17] that the updating must not be too quick to prevent numerical instability. Even in these kind of problems, stochastic methods are appropriate alternatives to find global solution using the penalty method. A constrained simulated annealing is developed in [14] and applied to a dynamic penalty function while a variant of the simulated annealing algorithm, the adaptive simulated annealing, is developed in [17]. Another heuristic is introduced in [18] that will use a temperature dependent penalty function in the simulated annealing cost function that is to be minimized. The aim of temperature dependent penalty function is to accelerate the simulated annealing convergence to the global optimum and to avoid premature convergence to a local optimal solution. Therefore, the penalty parameter is dependent on the temperature and is cooled with the temperature in the minimization problem. In [18], the penalty method is applied to solve a Block Angular Form reduction problem. However, it can be used to solve many other kinds of optimization problem such as the knapsack problem.

The knapsack problem (KP) is a constrained NP-complete optimization problem. In this problem, we have a set of items, each with their own weight and value. The objective is to find the maximum sum of values that can be put in the knapsack, knowing the summation of the weights in the knapsack must not exceed the maximum weight allowed. This problem can be formulated as follow:

$$(\mathrm{KP}): \quad \max_{x_i} \quad \sum_{i\in[1,n]} v_i x_i \qquad \text{subject to} \quad \sum_{i\in[1,n]} w_i x_i \le W \qquad x \in \{0,1\} \quad \forall i \in [1,n]$$

Where n is the number of items, v_i and w_i respectively the value and the weight of the item number i and W is the maximum weight.

Penalty functions, as explained in [20], are effective to solve this kind of problems. In the approach presented, different penalty functions are employed and tested to adjust the objective function using a genetic algorithm to solve the problem without constrains obtained by using the penalty method. Indeed, there are many variations of the knapsack problem in business and industrial application, and it would be interesting to have an effective resolution method. Task scheduling can be seen as an application of the knapsack problem. Indeed, it is possible to associate the values v_i of the knapsack problem with collection slots or machine availability times, and the maximum weight allowed W with the schedule time where the machine can be available or not. In [21], fully polynomial approximation schemes are designed to solve a knapsack problem. It is demonstrated that the method can be adopted for machine scheduling problems. In the scheduling applications, the machines need to process multiple jobs which takes a certain duration knowing that there are some amounts of time when the machine is subjected to a maintenance. The article also looks at different scenarios such as the version where the sum of the weighted completion time on a single machine with a fixed machine non-availability interval is to be minimized.

Simulated Annealing algorithm overview

Simulated Annealing (SA) is a metaheuristic method for global optimization problems. It is based on the physical phenomenon of annealing of materials. In metallurgy, there are two steps for physical annealing: first, the solid is heated to a very high temperature (until it glows) and then, it is slowly cooled to room temperature.

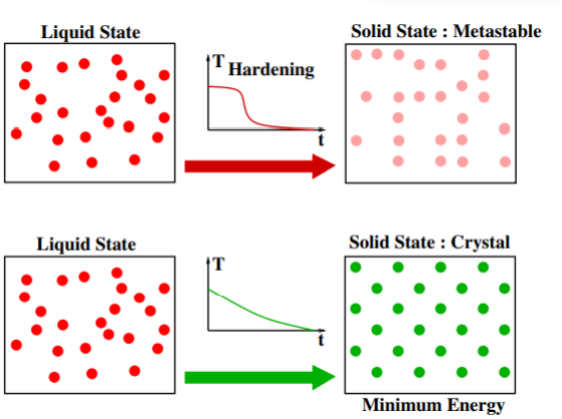

Figure 1 - Visualization of the state of the material and how we can lower temperature to cool it [22]

It can be seen in Figure 1 that when the temperature drops too quickly, the state ends in a metastable state whereas when the temperature drops slowly, the atoms in the solid are well organized. The aim is to make the material reach a solid state where all atoms are symmetrically organized. In the algorithm, the state-space point represents the different states of the solid and the function to minimize represents the energy of the solid. Thus, in the metastable state, the objective function will not be well minimized while in the crystal state the minimum energy will be reached, and the objective function will be minimized.

SA algorithm, as it can be seen in [22], is based on Monte Carlo algorithms and is an adaptation of the Metropolis Algorithm [19]. The Monte Carlo algorithm is a local search algorithm used to optimize a cost function. It converges to local optima whereas the Metropolis algorithm uses a criterion in order to escape from local minima.

The principle of the SA algorithm is to try to approximate the global minimum of a given function. An initial state X_{init} of energy E_{init} is generated. This initial state is taken randomly and corresponds to an initial temperature $T = T_{init}$ that is high and arbitrarily selected. Then, another state X_j of energy E_j is generated. This other state can be accepted according to the Metropolis criterion. By looking through the probabilistic theory, the probability that the solid is in the state X_i of energy E_i at the temperature T is given by: $exp(-E_i/k_BT)$ where $k_B = 1.38064852 \times 10^{-23}$ m^2 kg s^{-2} K^{-1} is the Boltzmann constant. Thus, the new state X_j is accepted if it decreases the energy of the system ($E_j < E_{j-1}$), and therefore minimizes the objective function, or it can be accepted with the probability $exp\left(-\left(E_{j-1} - E_j\right)/k_BT\right)$. This means that it is accepted to degrade the solution not to fall into a local maximum solution in order to find the global maximum of the function. Therefore, at every iteration, the state can be modified. Moreover, the

temperature T is continuously lowered and if this temperature reaches a threshold low enough or if the system does or change during multiple iterations, the algorithm stops.

Temperature plays a crucial role. At high temperature, the system is free to move in the state space by choosing states that do not necessarily minimize the energy and so the objective function. On the contrary, at low temperature, changes are less free to move. Therefore, the algorithm can allow state modification that increases the objective function or not to prevent the algorithm from falling into local maximum.

Application of the Simulated Annealing algorithm to data collect planning

The algorithm takes as an input the predicted number 1-Hz observation of low-elevation satellites (below 10°) for each 5-min slots in a given day. The GNSS satellite elevation is based on the computation of the satellite position from the broadcast navigation message [23] from the previous day, accessed through recorded RINEX navigation files. In the following, we will refer to the number of low-elevation satellites in 5-min slot as the number of samples.

The aim of this part is to optimize collection times in order to maximize the number of samples (or satellites seen at low elevation) while taking into account the processing time of the different collections. Indeed, the software receiver chosen for the data collect cannot, at the same time, collect data and process them to generate the multi-correlator outputs due to the high number of correlator outputs. In the end, the optimization algorithm will return a binary vector where the value 1 in the vector means that the receiver has to collect data for five minutes and the value 0, that it must not collect. During this time, when the element in the vector is equals to 0, the receiver can process data or stay idle.

Therefore, the aim is to maximize the number of samples by ensuring that the number of times when the software receiver collects and processes data at the same time is equals to 0. Moreover, all this process should be finished within the total data collect duration, set to one day, which means that data cannot be processed after the start of the following day. Then, this problem can be seen as a knapsack problem where the maximum weight allowed would be assimilated to the maximum number of 5-min slots that exist in 1 days, and the values to number of samples for each slots. To satisfy every condition of the problem, an algorithm using the penalty method is used, turning the constrained optimization problem into an unconstrained one.

The parameters of the problem are:

- $N = 288$ the number of 5-min slots in a single day
- $x_i = \begin{cases} 1 & \text{if the receiver collects data during the slot number } i \\ 0 & \text{otherwise} \end{cases}$
- v_i is the value associated to x_i. It is actually the number of samples in the slot number i
- $y_i = \begin{cases} 1 & \text{if the receiver processes data during the slot number } i \\ 0 & \text{otherwise} \end{cases}$

We assume that the post-processing duration is equal to the data collection duration, and that the post-processing of a data collect has to be performed just after the data collect.

We assume that the data is processed just after the data is collected. It is assumed that it takes the same amount of time for the receiver to collect data or to post-process it. Therefore, the vector y_i is defined from x_i.

The problem can be formulated as follow:

$$\begin{aligned} \max \quad & \sum_{i \in [1,N]} v_i x_i \\ \text{subject to} \quad & (1) \ \sum_{i \in [1,N]} x_i y_i = 0 \\ & (2) \ y_i = 0 \quad \forall i > N \end{aligned}$$

The first constraint ensures that the collection and the processing are not done at the same time. The second one ensures that the receiver is not collecting or processing data after the end of the data collect.

Let us call s_1 the objective function that we want to maximize: $s_1 = \sum_{i \in [1,N]} v_i x_i$, and s_2 the measure of the violation of the constraints (1) and (2): $s_2 = \sum_{i \in [1,N]} x_i y_i + \sum_{i > N} y_i$

To solve the problem, a model based on the penalty method is used. The penalty function is then the multiplication of a penalty parameter, that is called β, by s_2, the measure of the violation of the constraints. The penalty function is then:

$$penalty\ function = -\beta \times s_2$$

This penalty function is equal to 0 when the constraints are not violated, and is non-zero where the constraints are violated. Then the objective s_1 needs to be maximized while the s_2 needs to be minimized and equal to zero in the end of the algorithm. The objective function to maximize, which corresponds to the energy E_n associated to a state in the SA algorithm description, is:

$$z = s_1 - \beta(n) \times s_2$$

where $\beta(n)$ is a penalty parameter and will be updated at every iteration n of our algorithm. Indeed, a dynamic penalty method is used to find a better solution faster.

The problem presented in this paper is solved using a Simulated Annealing algorithm applied to the resolution of problems based on the penalty methods.
In this optimization problem, the first thing is to make sure that s_1 is well maximized before ensuring that the constraints are not violated. Therefore, in the maximization problem, the penalty parameter $\beta(n)$ evolves as the opposite of the temperature T, the crucial parameter used in the Simulated Annealing algorithm that was previously described. It helps accelerating the simulated annealing convergence to the global optimum and also prevents numerical instability as the update does not change too quickly since the temperature in the simulated annealing decreases slowly. A scale factor is also added to consider the potential scale difference between s_1 and s_2. In our problem, it is equal to:

$$\beta(n) = \left(1 - \frac{T(n)}{T_{init}}\right) \times 1000$$
$$T(n) = T_{init} \times 0.999^n$$

The initial temperature is chosen sufficiently high in order to establish the annealing process. Initially, s_2 is not consequent compared to the s_1 (the parameter $\beta(n)$ is equals to 0) and while maximizing the objective function, the value of s_1 is maximized with higher priority than the minimization of s_2 and thus, the number of samples is maximized. Then, as the temperature lowers continuously, the importance of s_2 in the objective function grows (as $\beta(n)$ grows) and the value s_2 is minimized with higher priority than the maximization of s_1. The value of s_2 is supposed to reach 0 so that the result will be without the violation of constraints.

Illustration of the optimized data collect planning process on a simple example

The proposed algorithm is illustrated on a simple case. The input sample vector is given in Figure 2, where only 15 observation slots are considered.

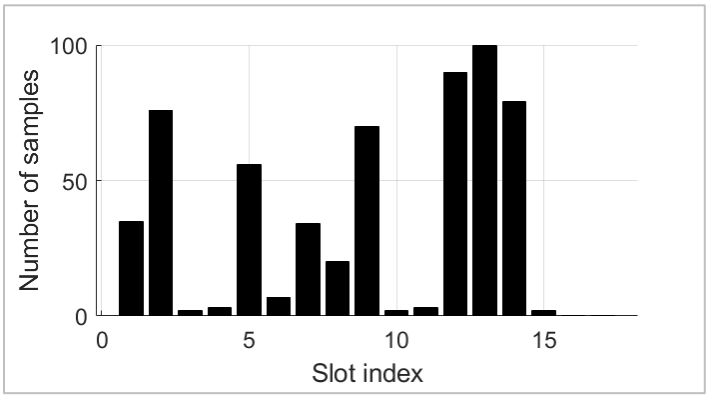

Figure 2 – Sample vector, corresponding to the number of 1-Hz observations from low-elevation satellites

The initial data collect vector (left on Figure 3) exhibits two constraint violations: (i) both data collect and data processing are running in slot 12, and (ii) the processing finishes 2 slots after the end of the data collects. When running the simulated annealing

algorithm, we obtain the final data collect vector (right on Figure 3), which has optimized the number of collected samples, while setting the constraint violation to zero.

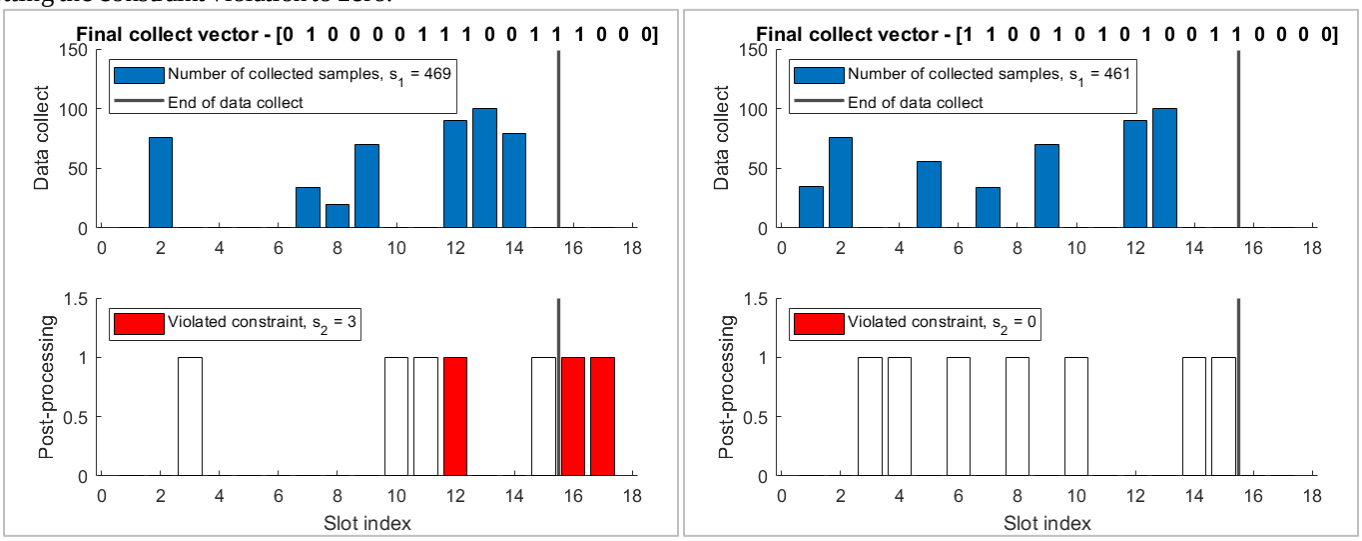

Figure 3 – Data collect instants (upper figures) and associated post-processing instants (lower figures). Red bars correspond to violated constraints. The final vector (right) corresponds to the optimized planning, which maximizes the number of collected samples while setting the constraint violation to 0.

Optimized data collect planning is one important part of the data collect automation, that permits to collect and process a large number of observations in a resource-constrained environment. This algorithm has been put in place in the data collect that has been running over several weeks, which is presented in the next section.

EXPERIMENTAL DATA COLLECT DESCRIPTION AND ANALYSIS

Data collect description

The data collect was set-up using a choke ring antenna located on the roof of an ENAC building, which should provide low multipath environment.

Figure 4 – Photos of the choke-ring antenna on the roof of an ENAC building

The automation of the data collect is described in Figure 5. It can be summarized as follow:

1. Automated data collection planning:
    a. retrieval of the ephemeris data from a RINEX FTP server
    b. elevation prediction
    c. optimized planning using the simulated annealing algorithm
2. Automated data collect (for each data collect)
    a. Create a configuration file
    b. Launch the recording of IQ samples
3. Automatic data post-processing
    a. Compute the correlator outputs from the IQ sample file
    b. filter the correlator outputs by elevation, to keep only low elevation satellites
    c. smooth the correlator outputs with a 25-s running average filter
4. Covariance matrix analysis
    a. update the covariance matrix computation using an iterative formula [16]

In step 3.a., it is possible to choose the number and location of correlators to be obtained, thanks to the flexibility of the software receiver. For this particular collect, the correlator outputs shown in were computed. Note that the number of correlators is much higher than what is used in actual SQM algorithm (see Table 2), which will be interesting for further research investigation.

Table 4 – correlator output location computed from the real data

	Correlator output delays (chips)
Galileo E1-C	± [0.01 0.02 0.03 0.04 0.05 0.06 0.07 0.08 0.09 0.10 0.11 0.12 0.13 0.14 0.15 0.16 0.17 0.18 0.19 0.20 0.30 0.40 0.50]
Galileo E5a-Q	± [0.1 0.2 0.3 0.4 0.5 0.6 0.7 0.8 0.9 1]

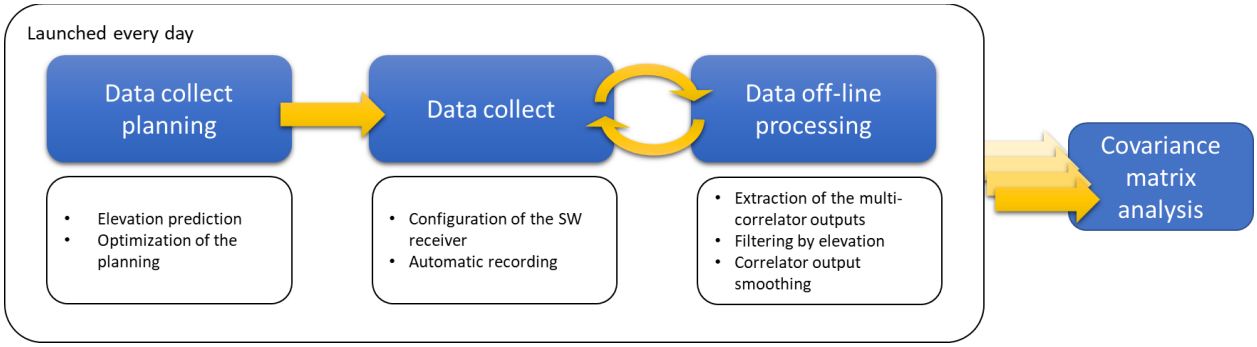

Figure 5 – Automated data collection and processing

After 30 days, we were able to collect 67,830 correlator outputs (at 1 Hz) for Galileo E1-C and E5a-Q signals received from low-elevation satellites. *(Note to the reviewers, the length of the data collect will change for the final submission, with the most recent data collect)*

Data Collect Analysis

The analysis of the collected data will only be performed for the Galileo E1-C signal.

Figure 6 show the standard deviation of the smoothed correlator outputs (normalized by the prompt correlator), as well as their correlation matrix obtained from the collected and post-processed data for Galileo E1-C for a single receiver (no averaging between several receiver). As a comparison, the same parameters obtained from the simulated data with parameters provided in Table 3 are also shown.

On Figure 6, the presence of multipath inflates the standard deviation for the correlator outputs associated to positive delays. Also, the level of the standard deviation is generally higher for most of the observed correlator outputs.
On Figure 7, the obtained covariance matrix of the correlator outputs is less smoothed with the observed data (left) than for the simulated data (right).

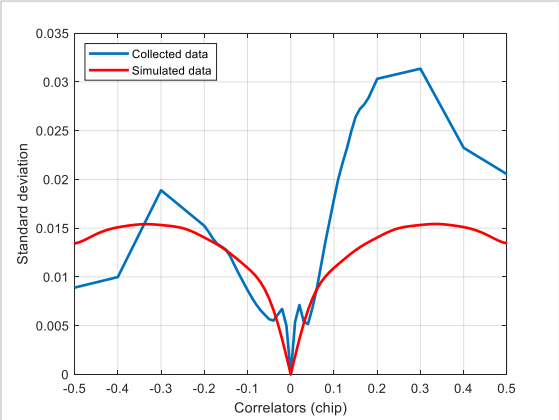

Figure 6 – standard deviation of the collected and simulated E1-C signals

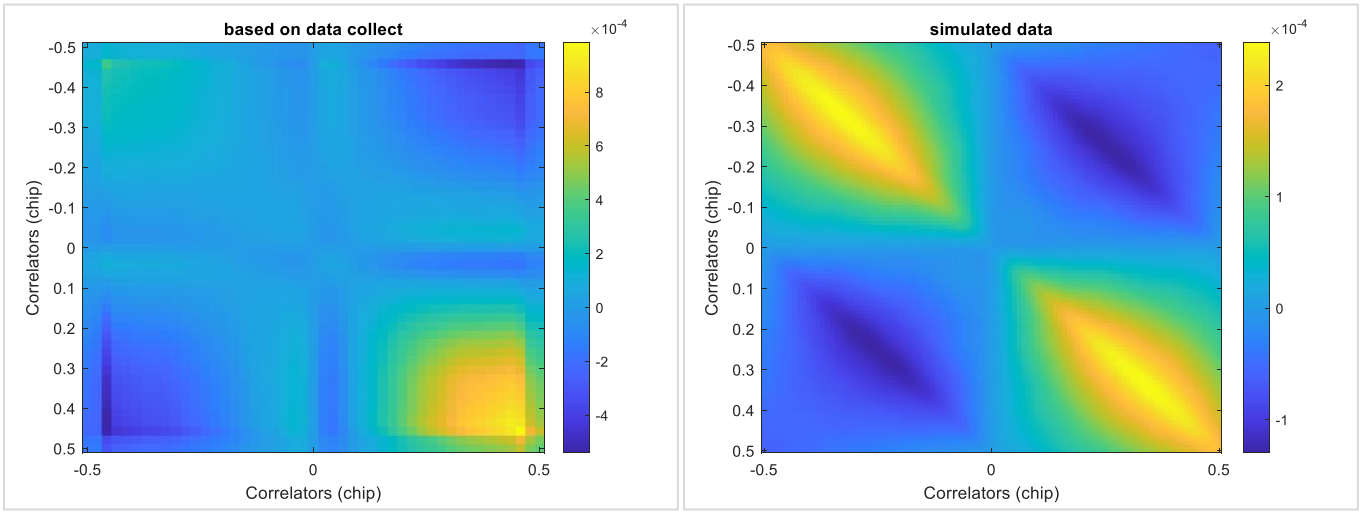

Figure 7 – Covariance matrix of the collected (left) and simulated (right) correlator outputs

SQM PERFORMANCE PREDICTION USING REAL DATA COLLECT

The SQM compliance performance is predicted thanks to a type of graph shown in Figure 8. Each circle of the graph corresponds to one distortion of the EWF Threat Space. The x-axis corresponds to the compliance test value. When it is above 1, it means that the distortion can be detected in compliance with the integrity requirements. The y-axis corresponds to the worst differential tracking error generated by the distortion among all possible airborne receiver configurations (pre-correlation filter type and bandwidth, and Early-Late correlator spacing). The red dotted line corresponds to the maximum tolerated error (aka MERR). All distortions leading to a differential tracking error larger than the MERR is required to be detected by SQM.

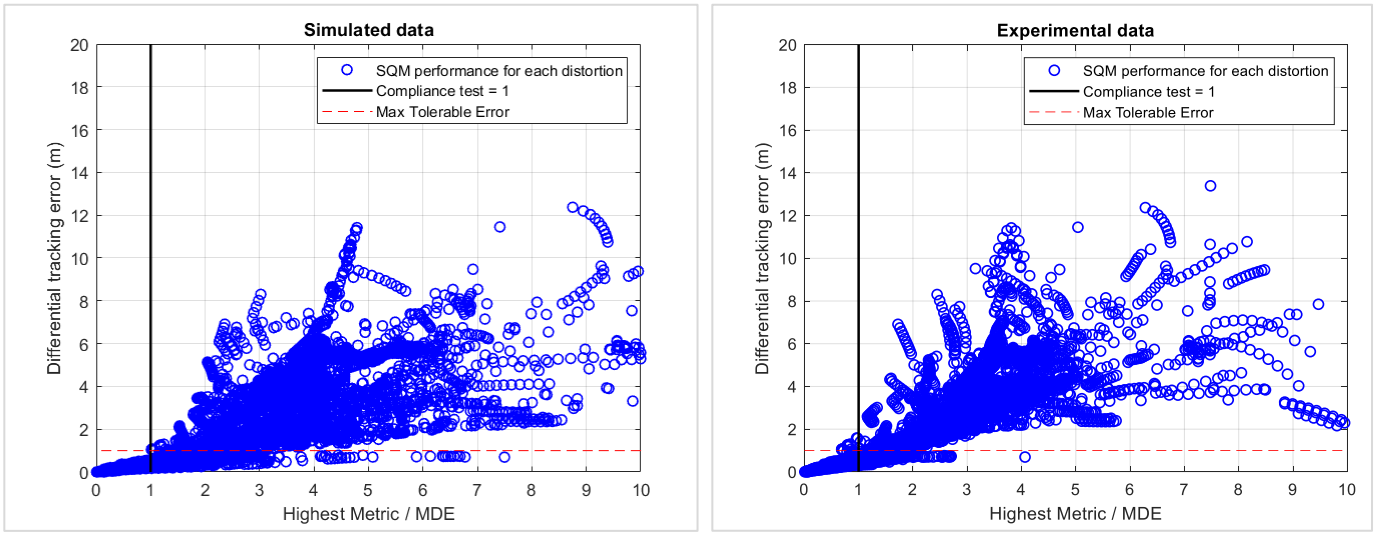

Figure 8 – SQM compliance prediction on simulated data (left) and experimental data (right)

Table 5 shows the predicted performances of the SQM algorithm for the various investigated cases. The simulated data show that the considered SQM algorithm, using a combination of single ratio, symmetric difference ratio and double difference ratio metrics using the correlator outputs of Table 2, exhibits a compliance of 100%.
While considering the real data, this value drops to 99.84%. This performance degradation is due either to the higher correlator standard deviation or to the higher covariance factor between them. The performance degradation is also visible just looking at the number of undetected distortions.

Table 5 – Predicted SQM performances using simulated data, experimental data and optimized SQM

	%age of undetected distortions	**%age of undetected distortions leading to a diff error > MERR**
Simulated model	9.62 %	0.00 %
Experimental data	13.11 %	0.14 %
Experimental data & optimized SQM	9.01 %	0.00 %

By exploiting the additional correlator outputs computed from the data collect (see Table 4), it has been possible to design a new SQM algorithm by choosing combinations of correlator outputs that are more sensitive to EWF distortions, while considering their particular distribution properties (standard deviation and covariance factor). Figure 9 shows the results obtained with the combinations of the correlators at the following location: ± [0.06 0.1 0.16 0.18 0.28 0.32 0.44 0.48]. This particular combination of correlators is just given as an example and shall not be considered as a definite result. Indeed, the choice of the correlator location highly depends on the receiving conditions of the signal (multipath presence, receiver tracking loop design).

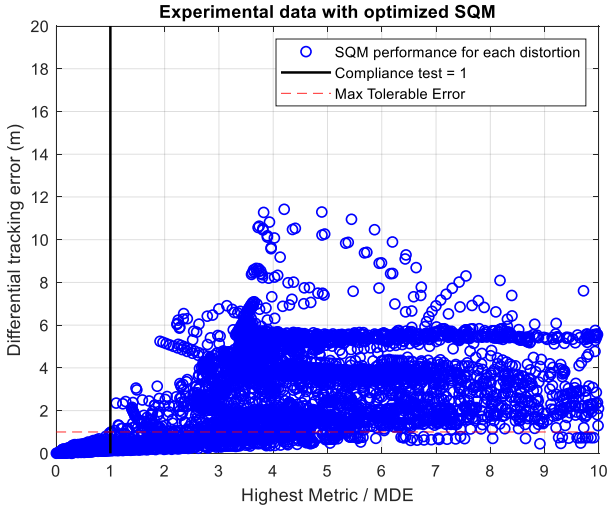

Figure 9 – SQM compliance prediction using experimental data and an optimized SQM algorithm

CONCLUSION

Signal Quality Monitoring is a process put in place in augmentation systems such as SBAS or GBAS to monitor potential signal distortions with high integrity that may be created by a satellite failure. It generally consists in the combination of several correlator outputs in so-called metrics, such as the single ratio metrics, the symmetric ratio metric or the double different metrics. To validate the compliance of a particular combination of metrics, it is necessary to validate the detection performance of an SQM process against every possible distortions of a Threat Space, in presence of typical errors affecting the metrics.

Usually, theoretical models are used in order to simulate the error affecting the correlator outputs and the metrics. However, those models cannot fully capture the diversity of the errors, such as the temporal correlation of multipath, or its effects on close correlator outputs. It is therefore of high interest to use real data collect in order to derive the models of the correlator output models, to validate the compliance of an SQM in operational conditions.

ENAC has put in place an automated data collect in order to observe the distribution of correlator output errors over a long period. Due to the large variation of the number of low-elevation satellites in a day, this scheduling task requires a specific process to collect as many observations as possible from low-elevation satellites in a limited period of time. An optimization algorithm, adapted from the simulated annealing process, allows to find an optimal scheduling, taking into account the constraint of the long post-processing task of the collected digitized samples by a software receiver.

By accumulating a large set of correlator outputs from low-elevation satellites, an accurate distribution of the covariance matrix of the correlator outputs is obtained, capturing all the effects occurring in the real world and in a real receiver. Applying th is distribution in the SQM compliance test show a degradation of the SQM performance, with potential integrity failures. However, this information can also be used in order to design an optimized set of SQM metrics, which minimizes the probability of integrity failures in presence of real errors on the correlator outputs.

Now that it is fully automized, the data collect will run for several months, which will provide previous information about on new GNSS signals that will be useful either to validate the performance of existing SQM processes, or to design new SQM metrics t ailored to the real observed errors at a given site.

ACKNOWLEDGMENTS

We would like to acknowledge the use of the IFEN SX3 software receiver and the Leica AR20 chokering antenna.

REFERENCES

1. ICAO, Annex 10 - Aeronautical Telecommunications, Volume 1 - Radio Navigation Aids, Sixth Edition., vol. 1. 2006.
2.
3. P. K. Enge, E. Phelts, and A. M. Mitelman, “Detecting Anomalous Signals from GPS Satellites,” 1999.
4. E. Phelts, T. Walter, and P. Enge, “Toward Real-Time SQM for WAAS: Improved Detection Techniques,” presented at the ION GPS/GNSS, Portland, Oregon, Sep. 2003.
5. M. Mabilleau, B. Kawak, M. Cordero Limon, S. Wallner, S. Spinelli, "Proposal for Galileo Evil Wave Form Threat Space," Montreal; 2018
6. I. Selmi, P. Thevenon, C. Macabiau, and M. Mabilleau, “Signal Quality Monitoring (SQM) Algorithm for Evil WaveForm (EWF) Threat Space (TS),” presented at the Navigation System Panel (NSP), Montreal, Oct. 2019.
7. J.B. Pagot, O. Julien, P. Thevenon, F. Amarillo-Fernandez, M. Cabantous, "Signal Quality Monitoring for New GNSS Signals," Navigation, Journal of the Institute of Navigation, 65(1), 2018.
8. J. Song, C. Milner, and I. Selmi, “Signal deformation fault monitors for dual-frequency GBAS,” NAVIGATION, vol. 67, no. 2, pp. 379–396, Jun. 2020.
9. J. Song, C. Milner, I. Selmi, S. Bouterfas, and O. Julien, “Assessment of Dual-frequency Signal Quality Monitor to Support CAT II/III GBAS,” Miami, Florida, Oct. 2019, pp. 508–519.
10. I. Selmi, P. Thevenon, C. Macabiau, O. Julien, M. Mabilleau, "Signal Quality Monitoring Algorithm Applied to Galileo Signals for Large Evil Waveform Threat Space," ION ITM 2020, 352–365, 2020.
11. P. Brocard, P. Thevenon, O. Julien, D. Salós, M. Mabilleau, "Measurement Quality assessment in urban environments using correlation function distortion metrics," ION GNSS+ 2014, pp. 2684–2697, 2014.
12. P. Shloss, R. E. Phelts, T. Walter, and P. Enge, “A Simple Method of Signal Quality Monitoring for WAAS LNAV/VNAV,” presented at the ION GPS, Portland, Oregon, Sep. 2002.
13. R. M. Freund, “Penalty and barrier methods for constrained optimization,” Lecture Notes, 2004.
14. B. W. Wah, Y. Chen, and T. Wang, “Simulated annealing with asymptotic convergence for nonlinear constrained optimization,” Journal of Global Optimization, vol. 39, no. 1, pp. 1–37, 2007.
15. Ö. Yeniay, “Penalty function methods for constrained optimization with genetic algorithms,” Mathematical and Computational Applications, vol. 10, pp. 45–56, 2005.
16. M. Schlueter and M. Gerdts, “The oracle penalty method,” Journal of Global Optimization, vol. 47, pp. 293–325, 2010.
17. A. I. Pereira and E. M. Fernandes, “Comparative study of penalty simulated annealing methods for multiglobal programming,” Proceedings of the 2nd International Conference on Engineering Optimization, 2010.
18. J. M. Stern, “Simulated annealing with a temperature dependent penalty function,” ORSA Journal on Computing, vol. 4(3), pp. 311–319, 1992.
19. I. Beichl and F. Sullivan, "The Metropolis Algorithm," in Computing in Science & Engineering, vol. 2, no. 1, pp. 65 -69, Jan.-Feb. 2000.
20. A. Olsen, “Penalty functions and the knapsack problem,” in Proceedings of the First IEEE Conference on Evolutionary Computation. IEEE World Congress on Computational Intelligence, pp. 554–558 vol.2, 1994.
21. H. Kellerer and V. Strusevich, “Fully polynomial approximation schemes for a symmetric quadratic knapsack problem and its scheduling applications,” Algorithmica, vol. 57, pp. 769–795, 2010.

22. D. Delahaye, S. Chaimatanan, and M. Mongeau, “Simulated annealing: From basics to applications,” Handbook of Metaheuristics, pp. 1–35, 2019.
23. "European GNSS (Galileo) Open Service Signal-In-Space Interface Control Document," Issue 2.0, 2021.
24. B. P. Welford. "Note on a Method for Calculating Corrected Sums of Squares and Products", Technometrics, 4:3, 419-420, 1962.